Arch. Metall. Mater. **63** (2018), 3, 1101-1108

DOI: 10.24425/123782

N. IZAIRI*#, F. AJREDINI*, A. VEVECKA-PFIFTAJ**†, P. MAKRESKI***, M.M. RISTOVA****

MICROHARDNESS EVOLUTION IN RELATION TO THE CRYSTALLINE MICROSTRUCTURE OF ALUMINUM ALLOY AA3004

Equal-channel angular pressing (ECAP) was used as a technique for severe plastic deformation (SPD) on Al alloy AA3004. This technique produced fully dense materials of refined grain structure to sub-micrometer dimensions and advanced mechanical properties. The ECAP processing of samples was conducted as 1 to 4 passes through the die at room temperature. We present the results of the studied homogeneity evolution with the ECAP treatment. Furthermore, a Scanning Electron Microscope (SEM) was used for examination of the microstructure changes in samples undergone from 1 to 4 passes. The microhardness-HV increased upon each ECAP pass. The resulting micro-hardness evolution was attributed to crystalline microstructure modifications, such as the d-spacing (studied by X-ray Diffraction-XRD) depending on the number of ECAP pressings. The microcrystalline changes (grain refining evaluated from the Scanning Electron Microscopy – SEM images) were found to be related to the HV, following the Hall-Petch equation.

*Keywords***:** Al alloy, AA3004, Equal-channel angular pressing (ECAP), microhardness, SEM, grain size, XRD

1. Introduction

During the past two decades, the equal-channel angular pressing (ECAP) along with the other severe plastic deformation (SPD) techniques have shown the possibility of producing ultrafine grain (UFG) structures in many metals and alloys [1-3]. Grain size reduction is one of the most attractive ways of improving the mechanical properties of metallic materials. Mechanical and physical properties of a crystalline material are determined by several factors, among which, the average grain size plays a crucial role. It is a well known that the strength of all polycrystalline material is related to the grain size (D) according to Hall-Petch equation (Eq. 1). This equation indicates that the strength of a metal (s) is equal to the frictional stress (σ_0) plus a factor (k) times the inverse of the square root of the grain size (D) [4]. Hence, reducing the grain size will cause the material to become stronger and its hardness increases (Eq. 1) [6,7].

$$\sigma = \sigma_0 + \frac{k}{\sqrt{D}} \tag{1}$$

Hence, the ECAP method holds a potential for grain refining and consequent strength improvement of the sintered materials [2-5]. This is especially related to the growing production of granular materials with extremely small grains. In principle, the shear strain imposed on the billet during ECAP is homogeneous [8,9] but in practice, the strain may be affected by several factors that lead to inhomogeneities in the internal microstructure [10-12]. Microhardness measurements represent a standard procedure for evaluating the strength and the level of homogeneity in samples processed to produce ultrafine grain sizes. By measuring the microhardness (HV) along linear traverses on the sample, it is possible to obtain quantitative information on the variations in the hardness and homogeneity on selected planes. In the last decades, several studies focused their examination on the mechanical behavior and the microstructural evolution of pure Al and Al-alloys processed by ECAP [13-17]. However, very little information is available about the evolution of microhardness and the degree of homogeneity along the orthogonal and longitudinal axes of billets processed by ECAP [16], although this information is crucial for the industrial application. Earlier investigations conducted on samples processed by either ECAP [19] or high-pressure torsion [18] demonstrated a direct correlation between microhardness measurements and the average grain sizes determined using transmission electron microscopy. Earlier reports described the evolution of homogeneity in the alloy Al-6061, where after 6 passes negligible increase in the microhardness is observed [20,22]. However, in our previous work, we have reported that the microhardness (HV) of the alloy A3004 [24] and AA5754 [25] improved with the number of ECAP passes. Also, other authors reported similar results of

* UNIVERSITY OF TETOVO, TETOVO, DEPARTMENT OF PHYSICS, FACULTY OF NATURAL SCIENCES AND MATHEMATICS, REPUBLIC OF MACEDONIA
** POLYTECHNIC UNIVERSITY OF TIRANA DEPARTMENT OF PHYSICS, TIRANA, ALBANIA
*** SS. CYRIL AND METHODIUS UNIVERSITY, INSTITUTE OF CHEMISTRY, FACULTY OF NATURAL SCIENCES AND MATHEMATICS, SKOPJE, REPUBLIC OF MACEDONIA
**** SS. CYRIL AND METHODIUS UNIVERSITY, INSTITUTE OF PHYSICS, FACULTY OF NATURAL SCIENCES AND MATHEMATICS, SKOPJE, REPUBLIC OF MACEDONIA
† DEACEASED SEPTEMBER, 2017
# Corresponding author: neset.izairi@unite.edu.mk

grain refinement on alloy AA3104 achieved by a hard pressure torsion (HPT) [26,27]. In the present work we offer a follow-up research of the microhardness evolution of AA3004 Al-alloy that was treated due to 0 to 4 ECAP passes under three different speeds of the plunger of the die (3, 4 and 5 mm/s), and an XRD analysis on the microcrystalline changes that occur during the ECAP processing. The 2θ values of the diffraction peaks from (111) and (200) planes were turned into the interplanar d-spacing, using the fundamental theory of diffraction known as Bragg's law ($n\lambda = 2d \sin\theta$, where λ is the wavelength of the incident X-rays, n is integer number). Also, from XRD results the strain was calculated.

2. Experimental part

The samples for ECAP treatment were sintered from AA3004 powder of 50 mm grain size in a shape of cylindrical rods with 10 mm in diameter. The preparation was a subject to different studies [16,24,25]. The AA3004 powder material before the sintering contained 97.8% A1, 1.2% Mg and 1% Mn. The ECAP deformation was performed at a room temperature through the route C [1,10], using L-banded channel die, as depicted in Figure 1. The samples were rotated for 180° about their longitudinal axis for every consecutive ECAP pass. The samples were inserted into the vertical channel of the die. Herein, the bending angle is $\Phi = 90°$ and the typical angle of the arch where two channels meet, $\Psi = 20°$ [24,25]. In ECAP processing the sample is pressed through the vertical channel of the die. Repetitive pressings were undertaken in order to improve the mechanical properties of the sample. The pressed samples emerged from the horizontal channel without experiencing any change in the cross-sectional dimensions. Each sample was then pressed with the plunger at the desired velocity, measured in mm/s. The walls of the die were lubricated to reduce the friction between the sample and the template.

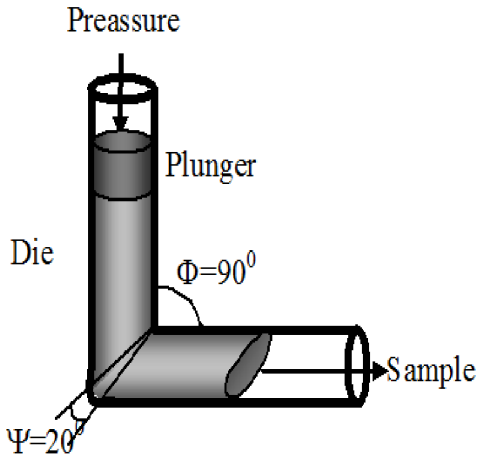

Fig. 1. Schematic view of an L-shaped ECAP die

The composition of the Al-alloy was determined with Scanning Electron Microscopy equipped with an Electron Dispersion Spectroscopy with Energy Dispersion Spectroscopy (SEM/EDS), using X-ray Microanalysis INCA X-act SN59444 instrumentation. The extruded samples upon the ECAP treatment were sliced in billets perpendicularly to their longitudinal axis Z. Also, all the microhardness tests were run in the transversal XY plane (Fig. 3).

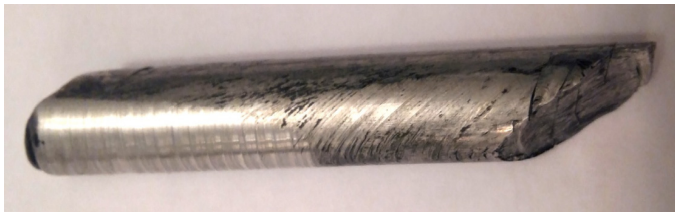

Fig. 2a. Photograph of the sample shape after ECAP passing

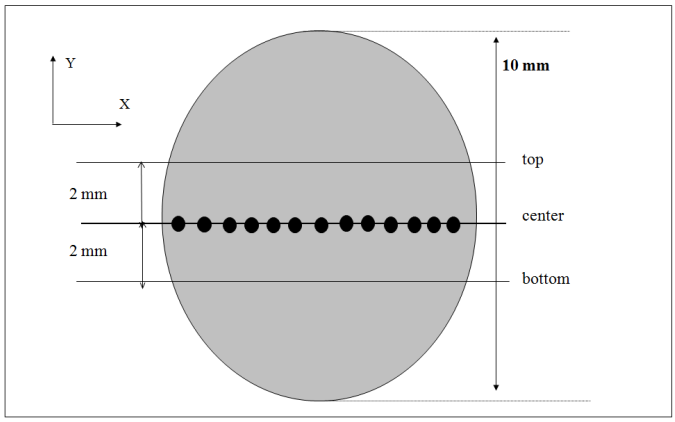

Fig. 2b. Simple diagram of HV measurement placement on the sample's XY cross-section

Each sample was prepared by careful polishing with a fine polishing paste until a mirror-like reflective surface was achieved. The standard microhardness measurements (HV) were performed on each sample, including the as-prepared sample (before ECAP pressing). Vickers HVS-30 Shimadzu equipment with a load of 200 g for the duration of 10 s was used to measure the microhardness. The HV measurements were performed along three parallel lines, one being the diametral line (center), while as the other two (top and bottom) were 2 mm apart on the both sides. The repeated measurements were made at a step of 0.25 mm (distance between the testing points), meaning that 17 HV measurements were made along each line (see dots presented on the line in the center in Fig. 2b).

The change in the morphology of the alloy was studied with a Scanning Electron Microscope, digitalized JEOL JSM-T220A system, although other, more sophisticated analytical techniques could be used, such as Transmission Electron Microscopy (TEM) and SEM with Electron Backscattered Diffraction SEM/EBSD [24]. The samples for the SEM were prepared in a cylindrical form pellets, 10 mm high and 10 mm in diameter. The sample surface was carefully polished with a gradual change of sand paper with granulation from 600 to 1200 and finished with a fine polishing paste. Finally, the mirror-like prepared surfaces were treated in 3% HF for 60-120 s, in order to obtain surface

abrasion/corrosion until distinct borders among the individual grains appear in the SEM image. X-ray Diffraction was used to study the microcrystalline changes in the material as a result of the ECAP pressings. For this purpose, a Rigaku Ultima IV X-ray diffractometer equipped with a high-speed detector system (D/teX *Ultra*) was used (CuKα radiation, $\lambda = 1.54056$ Å, 2θ range from 5° to 90°, accelerating voltage of 40 kV and anode current 40 mA). The samples for the XRD measurements were prepared from 2 mm thick sliced pallets, polished and rinsed before their examination. Also, the crystallite size of the ECAP passed alloys was estimated using the Scherer's equation.

3. Results and discussion

The Energy Despersive Spectroscopy (EDS) quantitative analysis was performed by sampling the spectra from four posts of the XY sample's surface, of which, two were distributed in the central part and other two on the periphery, as shown in Figure 3a. The SEM/EDS composition for each sampling posts is given in Figure 3b. The calculated mean quantity (from the four Spectra) of each element in weight percents was found to be: 92.86% Al, 4.07% Mg, 2.27% Mn, 0.6% Si, and 0.2% Cu. The differences in the composition compared to the precursor (the non-sintered powder alloy AA3004) depend on selected sampling posts (Spectrum 1, Spectrum 2, Spectrum 3 and Spectrum 4). Also, the presence of the new elements could be explained by the contamination of the samples with Si and Cu from the sintering and/or the ECAP equipment.

Figure 4a-d present the *HV* measurements on samples treated upon 1, 2, 3 and 4 ECAP passes in the die. Figure 4 also presents the *HV* values of the non-pressed sample (ECAP x0). Two apparent features are evident from Fig. 4: (i) mean *HV* increases after each ECAP's pass, and (ii) measured *HV* values are higher along the central line in comparison to those along the top or bottom lines. In addition, *HV* values are homogeneous in the central region of the sample. These results confirm that the ECAP processing provides good homogeneity with respect to the microhardness along the transversal plane. Further improvement in homogeneity is expected with the additional increase in the number of ECAP passes [23].

Figure 5 represents the evolution of the mean *HV* with the ECAP pressings. Herein, the values for the mean *HV* were calculated from the measurements from Figure 4. From Figure 5 it is clear that *HV* increased approximately by a factor of 2 after x2 ECAP passes (speed 3 mm/s). It is also evident that after the further passes (3 and 4) the *HV* slowly grows. These trends are generally consistent with the previous data for strength measurements [25]. In a similar manner, two series of *HV* measurements were made on the samples produced by ECAP (x1. x2, x3 and x4 passes) under two other different plunger speeds, 4 mm/s, and 5 mm/s. Also, it is evident that after 4 ECAP passes the plunger speed does not influence the value of the microhardness.

SEM images (Fig. 6a) depict the grain refining of the samples as a result of the ECAP passes. The average grain size (D) was evaluated upon each ECAP, by applying the linear approximation method using the HGS software on the SEM images and the scanning probe image processor (SPIP) for statistical analysis. The grain size measurements from the SEM images from Fig. 6a were presented as histograms revealing a normal distribution of the frequency of appearance of the grains, sizing 0-26 micrometers (step 2 µm), as shown in Fig. 6b.

From Fig. 6b it is obvious that the grain size population reveals normal distributions, where the dominant (maximum) grain size in the structure decreases from about 13 µm (for x1 ECAP pass) to about 4 µm (for the sample deformed by x4

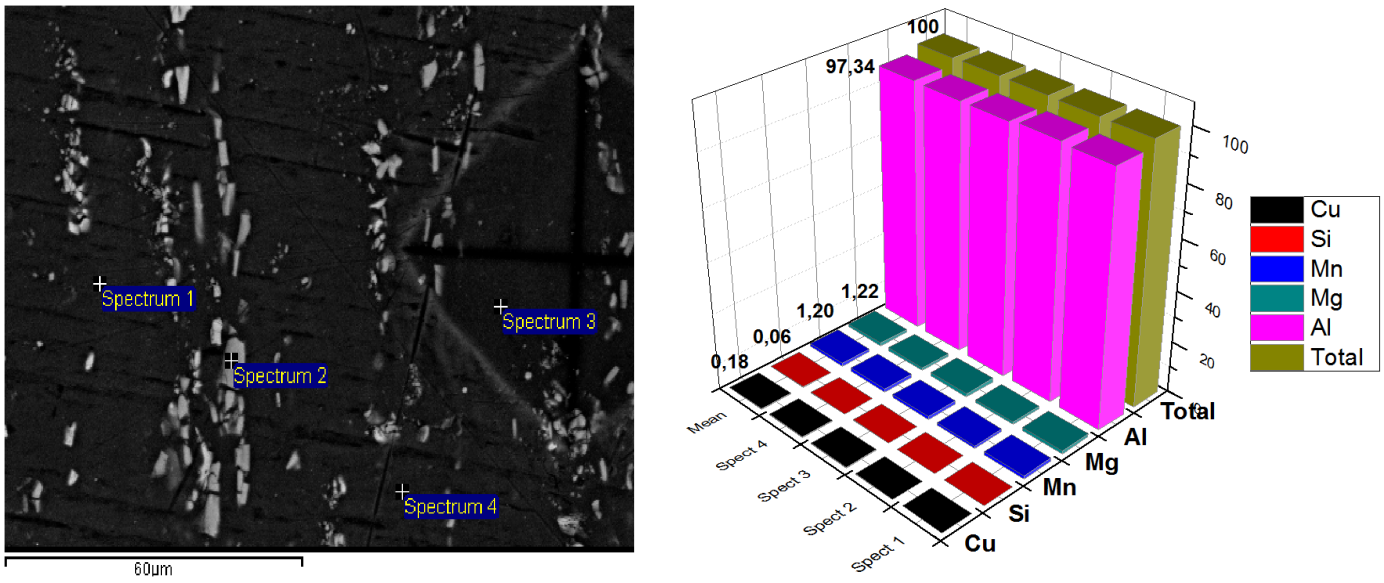

a) b)

Fig. 3. EDS quantitative analysis of AA3004 samples. The mean elemental composition of the sample is 92.86% Al, 4.07% Mg, 2.27% Mn, 0.6% Si, and 0.2% Cu: (a) EDS Spectra sampling posts and (b) EDS quantitative analysis

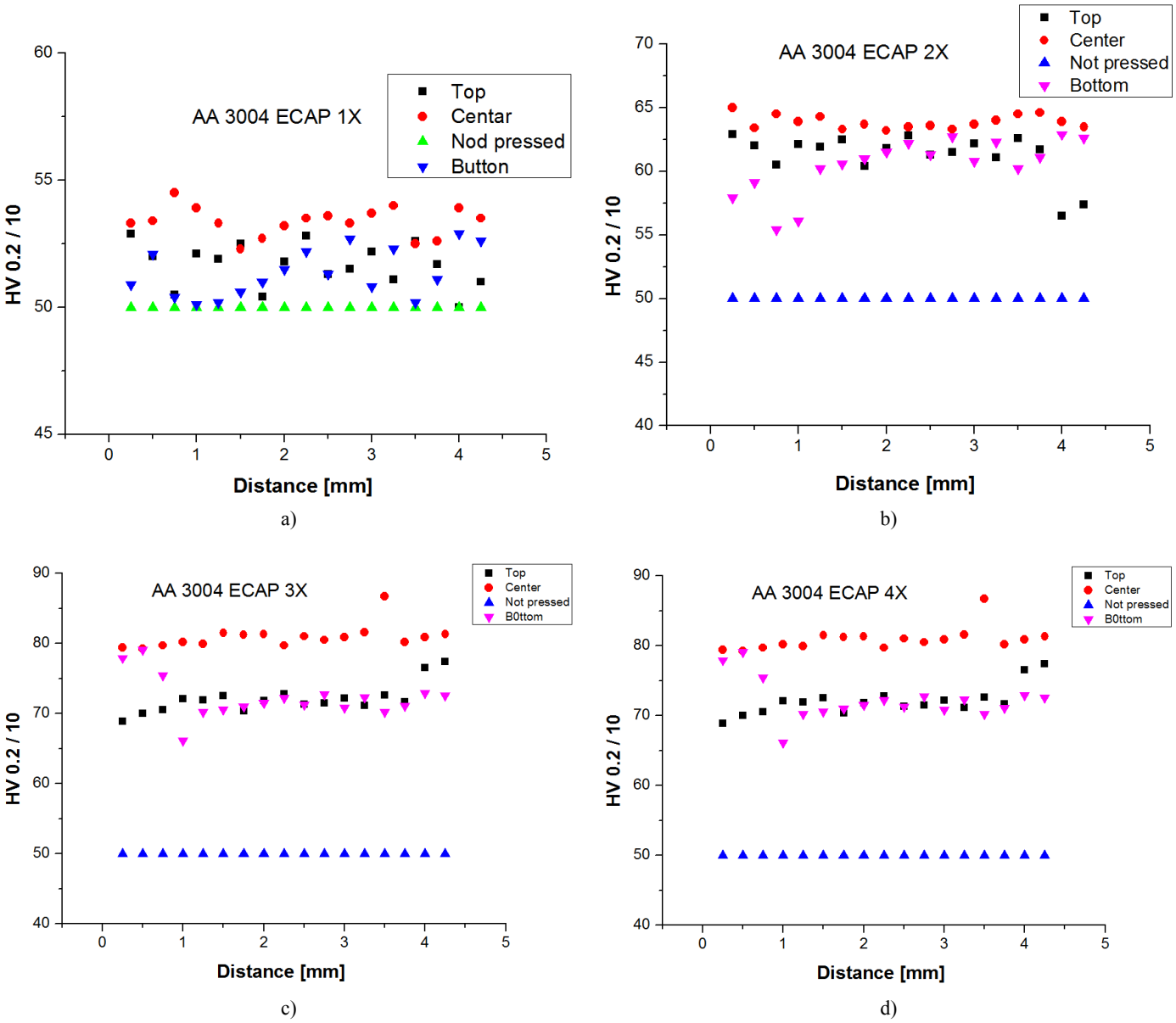

Fig. 4. Microhardness measurements of AA3004 after 1 to 4 ECAP passes performed under the speed of the plunger = 3 mm/s

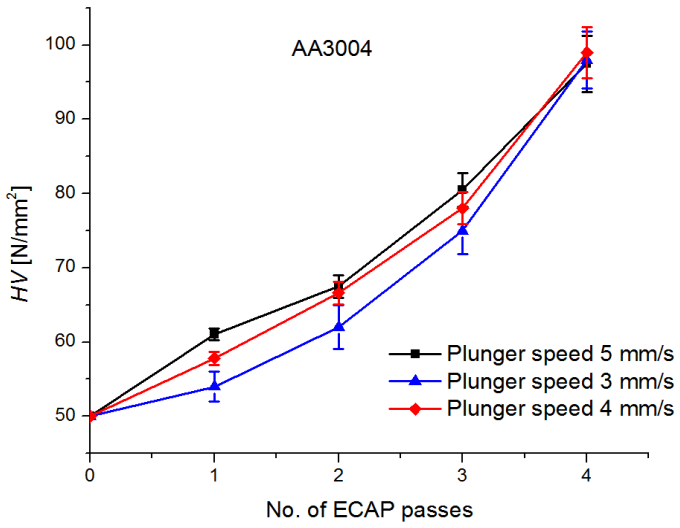

Fig. 5. *HV* (Vickers microhardness) evolution *vs*. ECAP passes for the samples produced under different plunger speeds

ECAP passes). However, other authors reported graphs that resemble log-normal distributions [26]. Figure 7 shows the grain size refining for the AA3004 samples treated by ECAP pressing for 1-4 times at three different speeds of the plunger. Obviously, the finest grain size was achieved at 4 mm/s speed of the plunger, which is considered to be the optimum speed for refinement purposes.

The first point (zero crossing) refers to the non-pressed sample (ECAP x0) where the grain size is ~50 μm (the granulation of the pre-sintering precursor [16]). It is clear that after 4 passes the mean grain size is reduced to ~5.0 μm. The mean grain size upon each following ECAP pass was calculated to be as follows: 11.6 μm (x1 ECAP), 10.4 (x2 ECAP), 9.0 (x3 ECAP) and 4.9 (x4 ECAP). From here it follows that the most effective grain refining occurred after 4 ECAP passes, being accompanied by an occurrence of a rapid evolution of the microstructure. Furthermore, from the SEM analysis, it is evident that early stage

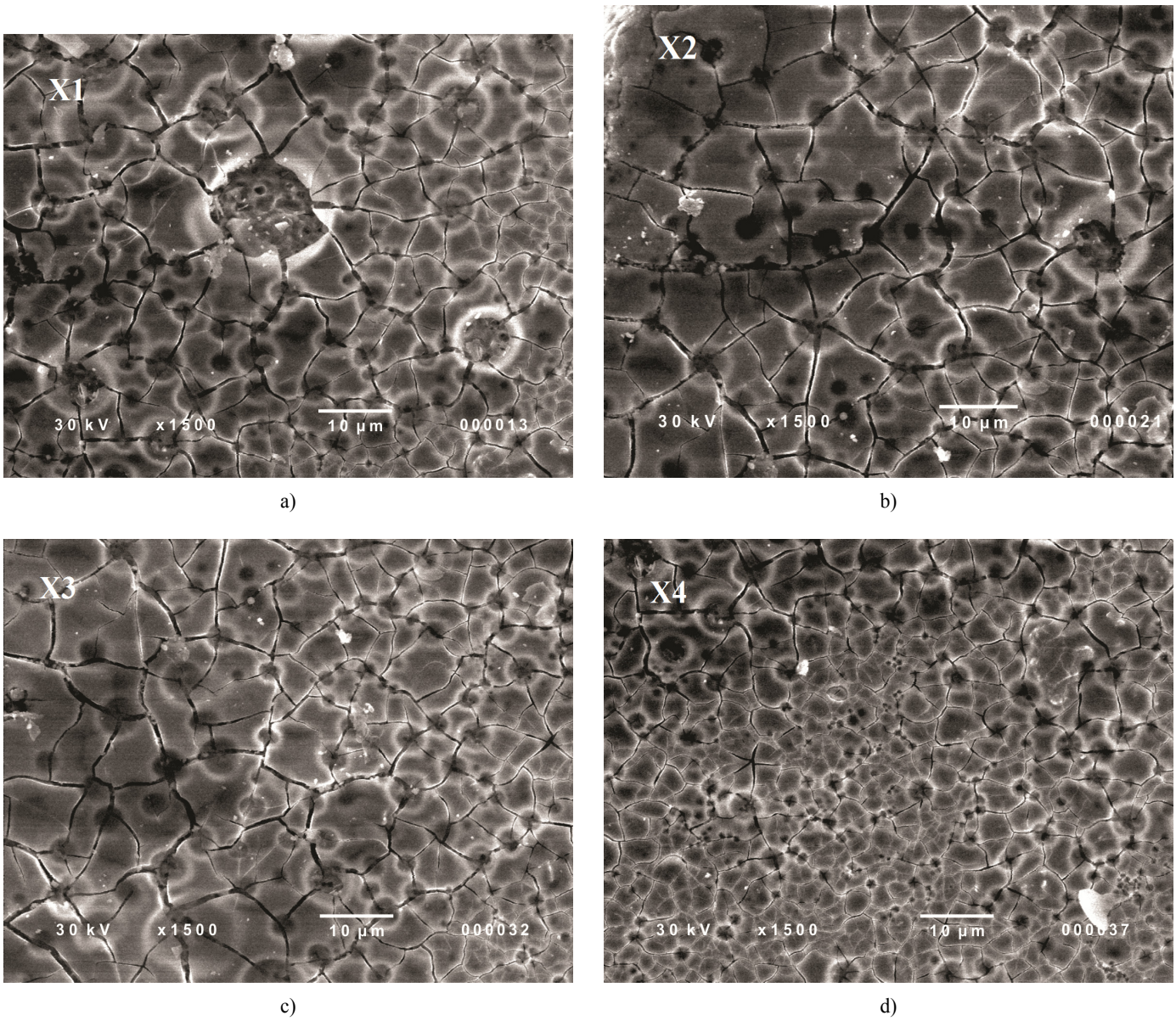

Fig. 6a. SEM Images on ECAP samples obtained through x1, x2, x3 and x4 ECAP presses (plunger speed = 3 mm/s)

room temperature recrystallization have not been observed: the grain refining progresses with each following ECAP processing.

In order to test whether the *HV* vs. *D* dependence is governed by the Hall-Petch equation (Eq. 1), we have presented $1/D^2$ changes on the horizontal axis, and HV on the vertical axis (Figure 8). As could be seen from Figure 8, the closest to a linear dependence (following the Hall-Petch equation) showed the samples subjected to a maximum of x3 ECAP deformations, treated under the plunger speed 4 mm/s. The plunger speeds at 3 and 5 mm/s revealed nonlinear dependence. Similar behavior was found for other Al-alloys treated by plastic deformation techniques [1,22].

Finally, the X-ray diffractograms (XRD) of AA3004 samples, treated by ECAP through x0 (unstrained sample), x1, x2, x3 and x4 passes are presented in Figure 9.

As could be seen from Figure 9, the concerning diffraction maxima are shifted towards higher 2q angles upon progressive ECAP passes, implying that the interplanar *d*-spacing slightly decreased upon repeated ECAP passes. Furthermore, the corresponding peak analysis showed that the crystallite size decreased inconsiderably, while as the mean strain practically remained unaltered upon the ECAP passes. The XRD results from the (111) and (200) peak analysis, and the calculated values of the *d*-spacing, crystallite size, and the lattice strain are given in Table 1.

From the mean values presented at the bottom of Table I at the bottom it could be seen that the ECAP deformation produced unstrained samples with inconsiderable deformation in the crystal lattice. The latter could be explained with the spatial rearrangement of the refined grains within the same volume as for the as-sintered sample (ECAP x0). In other words, the smaller grains fill up space more economically. Hence, the crystal lattice shows negligible deformation.

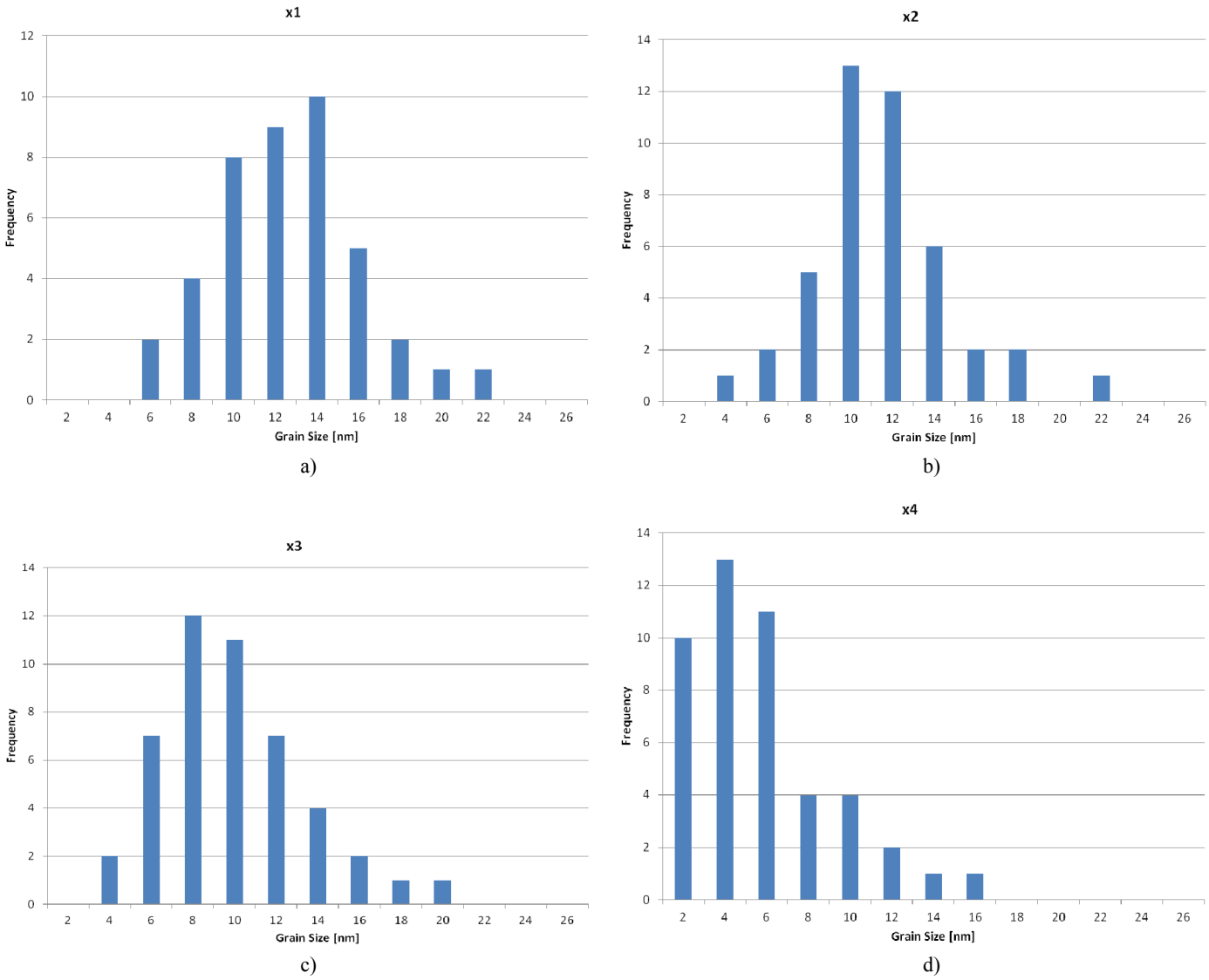

Fig. 6b. Histograms of the grain sizes population, depending on the number of ECAP passes (x1, x2, x3 and x4), measured and calculated from SEMs on Fig. 6a

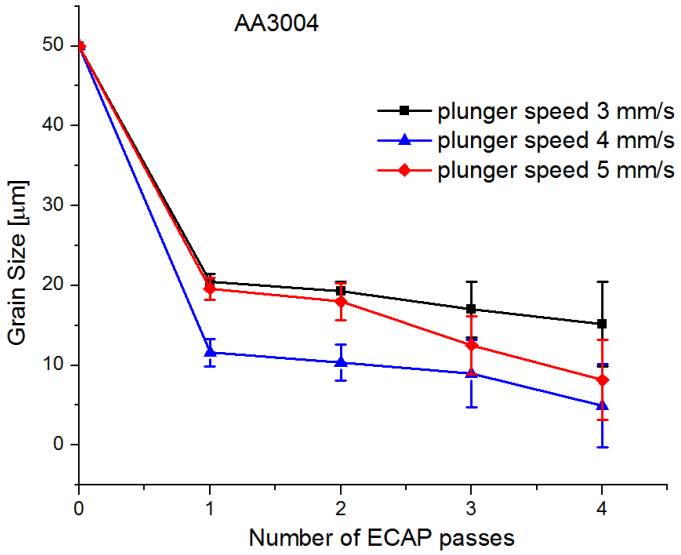

Fig. 7. Dependence of grain size (D) on the number of ECAP passes for AA3004 samples passed at three different Plunger speeds through the die

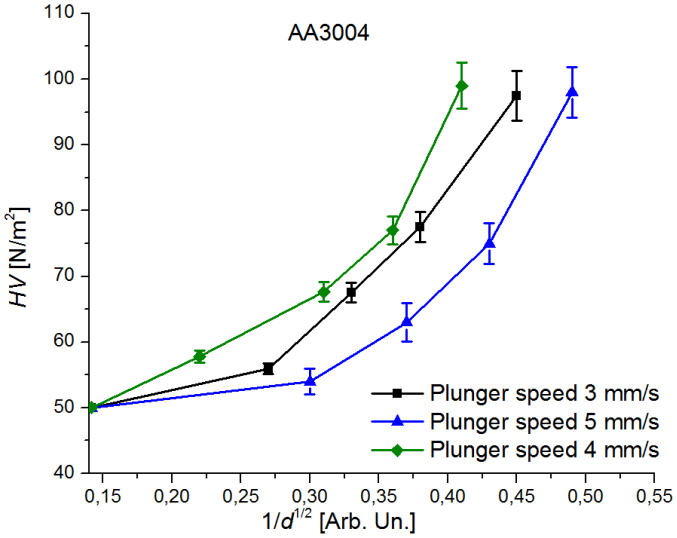

Fig. 8. Microhardness (HV) evolution as a function of the grain size (D)

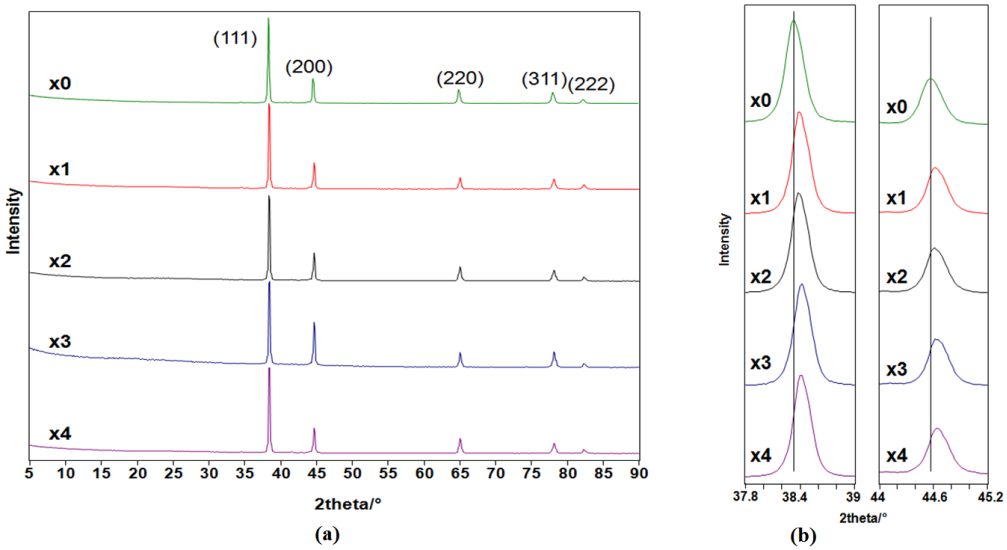

Fig. 9. (a) XRD patterns of AA3004 billets treated by ECAP through x0 (unstrained sample), x1, x2, x3 and x4 passes. (b) The obvious shift of the typical diffraction maxima of Al metal at (111) and (200) planes upon ECAP passes

TABLE 1

XRD data and peak analysis of x 0 (unstrained), and x 1, x 2, x 3 and x 4 ECAP samples

I – Data from (111) peak analysis from figure 9b					
ECAP	2q [degrees]	*d* [Å]	FWHM	Crystallite size [nm]	Strain
x0	38.338	2.348	0.219	40.16	0.0027
x1	38.405	2.344	0.221	39.81	0.0028
x2	38.397	2.344	0.224	39.27	0.0028
x3	38.431	2.342	0.229	38.42	0.0029
x4	38.420	2.343	0.226	38.93	0.0028
I – Data from (200) peak analysis from figure 9b					
x0	44.585	2.032	0.273	32.89	0.0028
x1	44.643	2.030	0.259	34.67	0.0028
x2	44.63	2.042	0.262	34.38	0.0028
x3	44.66	2.029	0.261	34.41	0.0028
x4	44.67	2.029	0.267	33.64	0.0028

ECAP	**x0**	**x1**	**x2**	**x3**	**x4**
Mean *d*-spacing from peaks I and II [Å]	2.190	2.187	2.187	2.186	2.186
Mean crystallite size from peaks I & II [nm]	36.53	37.24	36.83	36.42	36.29
Mean strain from peaks I & II [%]	0.275	0.280	0.280	0.285	0.280

4. Conclusions

ECAP appeared to be an effective tool for achieving a substantial reduction in the grain size of the commercially produced AA3004. Microstructural SEM image analysis showed that the grains underwent drastic refining upon the ECAP size from the initial ~50 μm down to ~5 μm after 4 ECAP passes. The most effective grain refining occurred after 4 ECAP passes, regardless of the speed of the plunger. The study showed that upon ECAP passing the grain size reduction induced significant improvement in the mechanical properties, such as the microhardness (*HV*). Similar results were obtained by other authors for other Al-alloys [2,22,25]. It was evident that the *HV* vs. *D* relation upon ECAP processing (maximum 3 passes) at 4 mm/s plunger speed is governed by the Hall-Petch equation. Furthermore, the XRD maxima revealed a shift towards higher 2q angles upon progressive ECAP passes, implying that the interplanar *d*-spacing reduced inconsequently. The analysis of the (111) and (200) peaks in the XRD patterns shows a petite decrease of the crystallite size upon the ECAP passes. As a final conclusion, the ECAP could be effectively used in the production of AA3004 with an improved mechanical and microstructure properties.

Finally, in our future studies, we should consider research on the inhomogeneous distribution of the HV or recrystallization at second phase particles in the deformed aluminum using the X-ray electron diffraction technique [28].

REFERENCES

[1] R.Z. Valiev, T.G. Langdon, Progress in Materials Science **51**, 881-981 (2006).

[2] M. Furukawa, Z. Horita, M. Nemoto, R.Z. Valiev, T.G. Langdon, Acta Mater. **44**, 4619-29 (1996).

[3] M. Kawasaki, Z. Horita, T.G. Langdon, Material Science and Engineering A **524**, 143-150 (2009).

[4] A. Loucif, R.B. Figueiredo, Th. Baudinc, F. Brisset, R. Chemama, T.G. Langdond, Materials Science and Engineering A 527, 4864-4869 (2010).

[5] A. Loucif, R.B. Figueiredo, Th. Baudinc, F. Brisset, R. Chemama, T.G. Langdond, Materials Science and Engineering A **532**, 139-145 (2012).

[6] O.E. Hall, Proceedings of the Royal Society B **64**, 747-753 (1951).

[7] N.J. Patch, Iron Steel International **174**, 25-28 (1953).

[8] Y. Iwahashi, J.Wang, Z. Horita, M. Nemoto, T.G. Langdon, Scripta Materialia **35**, 143-145 (1996).

[9] A. Vevecka, P. Cavaliere, M. Cabbibo, E. Evangelista, T.G. Langdon, Journal of Materials Science Letters **20**, 1601-1603 (2001).

[10] R.Z. Valiev, I.V. Islamgaliev, I.V. Alexandrov, Progress in Materials Science **45**, 103-189 (2000).

[11] V.M. Segal: Material Science and Engineering A **271**, 322-333 (1999).

[12] T. Kvackaj, J. Bidulska, M. Fujda, R. Kocisko, I. Pokorny, O. Milkovic, Materials Science Forum **633-634**, 273-302 (2010).

[13] T. Kvackaj, R. Kocisko, J. Bidulska, R. Bidulský, J. Dutkiewicz, Chemicke Listy **105**, 514-516 (2011).

[14] T. Kvačkaj, R. Kočiško, I. Pokorný, J. Bidulská, M. Kvačkaj, A. Kováčová, R. Bidulský, L. Litynska-Dobrzynska, J. Dutkiewicz, Acta Physica Polonica A **122**, 557-560 (2012).

[15] R. Bidulsky, J. Bidulska, M. Actis Grande, Chemicke Listy **106**, 375-376 (2012).

[16] A. Vevecka- Priftaj, A. Böhner, J. May, H.W. Höppel, M. Göken, Materials Science Forum 741, 584-586 (2008).

[17] T.G. Langdon, Materials Science and Engineering A **462**, 3-11 (2007).

[18] C. Xu, S. Schroeder, P. Berbon, T.G. Langdon, Acta Materialia **58**, 1379-1386 (2010).

[19] M. Prell, C. Xu, T.G. Langdon, Materials Science and Engineering A **480**, 449-455 (2008).

[20] S.N. Alhajeri, N.Gao, T.G. Langdon, Materials Science and Engineering A **528**, 3833-3840 (2011).

[21] S.L. Semiatin, D.P. DeLo, E.B. Shell, Acta Materialia **48**, 1841-1851 (2000).

[22] M.A. Meyers, A. Mishra, D.J. Benson, Progress in Materials Science **51**, 427-556 (2006).

[23] C. Xu, M. Furukawa, Z. Horita, T.G. Langdon, Materials Science and Engineering A **398**, 66-76 (2005).

[24] N. Izairi, F. Ajredini, A.Veveçka-Priftaj, M. Ristova, Materials and Technology **48**, 385-388 (2014).

[25] N. Izairi, F. Ajredini, M. Ristova, A. Vevecka-Priftaj, Acta Metalurgica Slovaca **19**, 302-309 (2013).

[26] H. Paul, A. Morawiec, T. Baudin, T. Czeppe, Archives of Metallurgy and Materials **60**, 131-144 (2015).

[27] H. Paul, T. Baudin, F. Brisset, A. Tarasek, Materials Science Forum **753**, 239-242 (2013).

[28] F.J. Humphreys, Acta Metallurgica **25**, 1323-1344 (1977).